Multiple antimagnetic rotation bands in odd-A ^{107}Cd

Deepika Choudhury,[1,*] A. K. Jain,[1] G. Anil Kumar,[1] Suresh Kumar,[2] Sukhjeet Singh,[3] P. Singh,[4] M. Sainath,[5] T. Trivedi,[6] J. Sethi,[6] S. Saha,[6] S. K. Jadav,[6] B. S. Naidu,[6] R. Palit,[6] H. C. Jain,[6] L. Chaturvedi,[7] and S. C. Pancholi[8]

[1]*Department of Physics, Indian Institute of Technology, Roorkee-247667, India*
[2]*Department of Physics and Astrophysics, University of Delhi, Delhi-110007, India*
[3]*Maharishi Markandeshwar University, Mullana, Ambala-133207, India*
[4]*Indian Institute of Technology Kharagpur, Kharagpur-247667, India*
[5]*Mahaveer Institute of Science and Technology, Hyderabad-500005, India*
[6]*Tata Institute of Fundamental Research, Mumbai-400085, India*
[7]*Guru Ghasidas University, Bilaspur-495009, India*
[8]*Inter University Accelerator Center, New Delhi-110067, India*

(Received 2 January 2013; published 6 March 2013)

Lifetimes of the excited states of a pair of positive-parity $\Delta I = 2$ bands of ^{107}Cd have been measured by using the Doppler-shift attenuation method. The obtained $B(E2)$ transition rates significantly decrease with increasing spin, a behavior typical of antimagnetic rotation (AMR). The observed results, interpreted by the semiclassical model (SCM) calculations, confirm these bands to be AMR bands resulting from the coupling of a pair of high-Ω $g_{9/2}$ proton holes to aligned $g_{7/2}(h_{11/2})^2$ neutron particles. This is the first evidence for two AMR bands in a single nucleus.

DOI: 10.1103/PhysRevC.87.034304 PACS number(s): 21.10.Tg, 21.10.Re, 21.10.Hw, 27.60.+j

I. INTRODUCTION

In analogy to the spin arrangement in antiferromagnetism, a unique proton-neutron spin coupling giving rise to rotationlike band structures in nearly spherical nuclei was proposed by Frauendorf [1]. Since then the phenomenon called the twin-shears mechanism or more commonly, antimagnetic rotation (AMR), has gained much scientific interest. In an anti-magnetic rotor, two angular momentum vector blades $\vec{j}_{\pi_1}$ and $\vec{j}_{\pi_2}$ of the proton holes (particles) are stretched apart, each coupled nearly perpendicular to the angular momentum vector $\vec{j}_\nu$ of a neutron particle (hole), such that the total angular momentum vector $\vec{I}$ is along $\vec{j}_\nu$ [2]. Such a neutron proton coupling gives rise to a $\Delta I = 2$ band with weak $E2$ transitions, a feature that makes the phenomenon interesting. The high spin states in an AMR band are generated due to the gradual closing of the proton blades towards the neutron angular momentum vector, i.e., by the gradual closing of the twin shears, driving the nucleus towards sphericity indicated by a gradual decrease in the reduced transition probability [$B(E2)$] values with increase in spin. By its very nature, the phenomenon is bound to be very rare and difficult to observe. Hence, there are very few confirmed cases of AMR found to date, resulting in a limited understanding of the concept compared to the well-established magnetic rotation (MR) phenomenon [3]. Firm experimental evidence of AMR in even-even nuclei has been reported in only three cases, namely, ^{106,108,110}Cd [4–7]. The first observation of AMR in an odd-A nucleus ^{105}Cd was recently reported by us [2]. The self-consistent microscopic calculation by Zhao *et al.* [8] further confirms our interpretation of AMR in ^{105}Cd. In this mass region, the high-Ω $g_{9/2}$ proton hole(s) and low-Ω $h_{11/2}$, $g_{7/2}$ neutrons are known to play an active role in the AMR mechanism.

Until now, only one AMR band has been observed in a single nucleus. In this paper, we present the first evidence of two AMR bands in one nucleus, viz. the odd-A ^{107}Cd. This is also the first evidence of a pair of signature partner bands showing AMR nature. The high spin states of ^{107}Cd were earlier studied by Jerrestam *et al.* [9]. We measured the lifetimes of the high spin states in the positive-parity bands 5 and 6 of ^{107}Cd using the Doppler-shift attenuation method (DSAM). The empirical $B(E2)$ values are interpreted using the semiclassical model (SCM) for AMR and the results confirm the AMR nature of the bands.

II. EXPERIMENTAL DETAILS

High spin states of ^{107}Cd nuclei were populated using the ^{94}Zr(^{18}O,5n) reaction at a beam energy of 85 MeV produced by the 15-UD Pelletron accelerator at the Tata Institute of Fundamental Research (TIFR), Mumbai. The target used was an isotopically enriched ^{94}Zr of thickness 0.9 mg/cm^2 on ^{197}Au backing of thickness 10 mg/cm^2. Short lifetimes ($\lesssim$1 ps) of the high spin states were measured using the DSAM technique. The deexciting γ rays were detected by using the Indian National Gamma Array (INGA) comprised of 18 Compton suppressed germanium clover detectors arranged in six rings, viz. 157°, 140°, 115°, 90°, 65°, and 40°, with respect to the beam direction [10,11]. Data were collected using a digital data acquisition (DDAQ) system based on Pixie-16 modules developed by XIA LLC [10–12] with the trigger set in the $\gamma - \gamma$ mode. After calibrating and gain matching the data with the analysis program DAMM [13], the $\gamma - \gamma$ events were sorted into $E_\gamma - E_\gamma$ symmetric and angle-dependent asymmetric matrices using the MARCOS program [14]. The RADWARE [15]

*deepika.chry@gmail.com

and LINESHAPE [16] analysis programs were used for further analysis of the data.

III. RESULTS

Figure 1 shows a partial level scheme of ^{107}Cd showing the positive-parity bands. The energies, intensities, and multipolarities of the transitions obtained from the present data mostly agree with the earlier published works [9], with some modifications and additions [17]. Using the angle-dependent asymmetric matrices (all vs 157°, all vs 140°, and all vs 40°), lifetimes of the states in the positive-parity bands 5 and 6 of ^{107}Cd were extracted by fitting the Doppler broadened line shapes of the corresponding in-band transitions. Simulating the slowing down of the recoiling nuclei in the target and backing, velocity profiles for the recoil were generated for groups of detectors at angles 157°, 140°, and 40° by using Monte Carlo methods with a time step of 0.001 ps for 5000

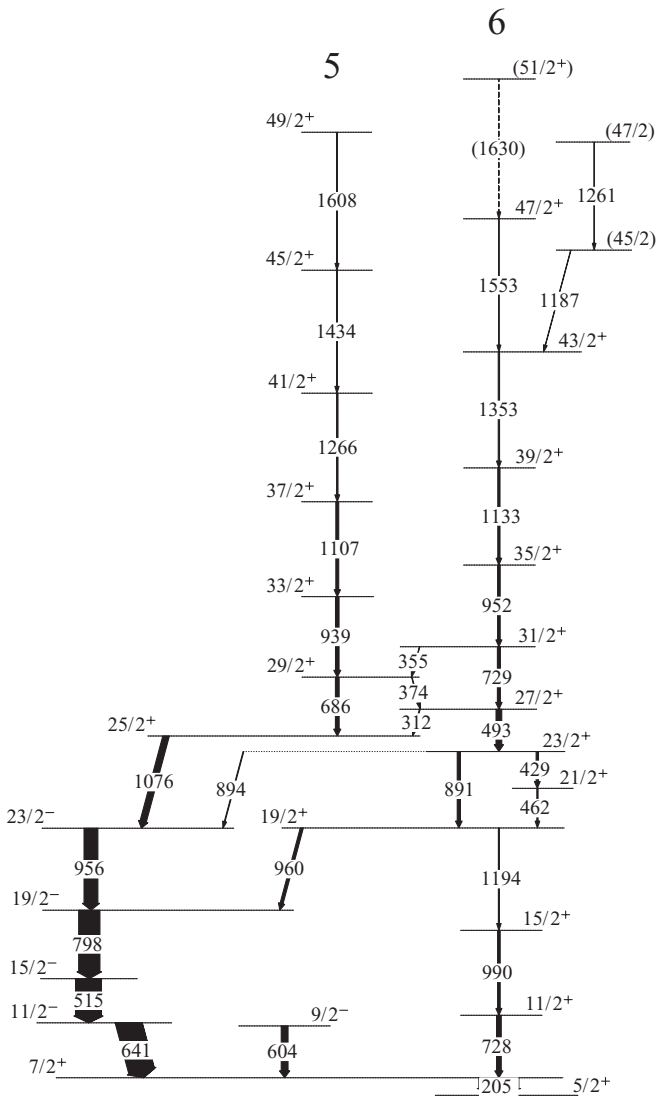

FIG. 1. Partial level scheme of ^{107}Cd showing the positive-parity bands 5 and 6.

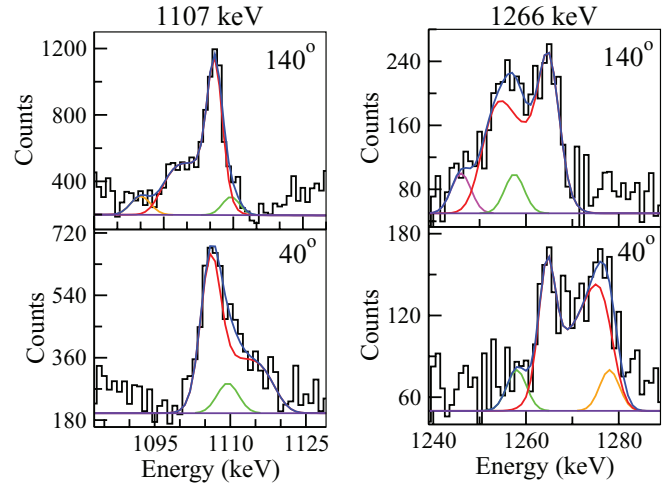

FIG. 2. (Color online) Representative spectra and the line-shape fits for the 1107-keV transition using the 1076 + 686 + 939 keV sum gated spectrum (left) and 1266-keV transition using the 686 + 939 keV sum gated spectrum (right). The true line shape of each peak is shown by the red line. The blue line shows the total fitting after including all the contaminant peaks (shown by the green, pink, and orange lines).

histories of energy losses at different depths. The electronic stopping powers of Northcliffe and Schilling, corrected for shell effects, were used to calculate the energy losses [2,18]. The energies of the decaying γ rays and the intensities of the side feedings into the states were used as input parameters for line-shape analysis [2]. Line shapes of each of the transitions were simulated and fitted to the experimental spectra using χ^2 minimization routines of MINUIT [19]. After minimizing the χ^2 value for each state individually, a global fit of the full cascade was performed to deduce the lifetimes of each of the states. The uncertainty in the lifetimes was determined from the vicinity of the minimum using the MINOS routine [19].

For band 5, we used the 686 + 939 + 1076 keV sum gated spectra for extracting the lifetimes of the levels from spin $37/2^+$ and the single 686-keV gated spectra for fitting the 939-keV peak ($33/2^+$ level). Line-shape fit of the 1107-keV transition energy is shown in Fig. 2. The lifetime of the $41/2^+$ level was further verified from the line-shape fits for the 1266-keV peak using the (686 + 939) keV sum gated spectra having fewer contaminant peaks (shown in Fig. 2). For band 6, we used the 493 + 729 keV gated spectra for the line-shape analysis of the transitions above spin $31/2^+$ and the 798-keV ($19/2^- \rightarrow 15/2^-$) gated spectra to extract the lifetime of the $31/2^+$ level. The 798-keV gate avoids contamination due to the low-spin 728-keV transition ($11/2^+ \rightarrow 7/2^+$). The lifetimes of the $35/2^+$, $39/2^+$, and $43/2^+$ levels were further verified by using the 960-keV gated spectra.

For both the bands 5 and 6, the deduced lifetimes (τ), $B(E2)$, and the quadrupole moment (Q_t) values along with their respective fitting errors are shown in Table I. The measured $B(E2)$ values decrease sharply with increase in spin for both the bands as shown in Fig. 3. The Q_t values and hence the quadrupole deformation β_2 also decrease with increase in spin for both these bands, as expected in the AMR mechanism.

TABLE I. Results of the line-shape analysis for the positive-parity bands 5 and 6 of ^{107}Cd. τ represents the mean lifetime of the state (I) deexciting by a γ ray of energy E_γ. $B(E2)$ is the corresponding reduced transition probability.

$E_\gamma(I)$ (keV)	$Q_t(eb)$	τ (ps)	$B(E2)(eb)^2$
Band 5			
$939.0(\frac{33}{2})$	$2.399^{+0.07}_{-0.06}$	$0.609^{+0.030}_{-0.035}$	$0.183^{+0.010}_{-0.009}$
$1106.6(\frac{37}{2})$	$2.175^{+0.04}_{-0.04}$	$0.317^{+0.012}_{-0.012}$	$0.155^{+0.006}_{-0.006}$
$1265.5(\frac{41}{2})$	$1.958^{+0.07}_{-0.09}$	$0.196^{+0.018}_{-0.014}$	$0.128^{+0.009}_{-0.012}$
$1434.0(\frac{45}{2})$	$1.668^{+0.06}_{-0.07}$	$0.142^{+0.012}_{-0.010}$	$0.094^{+0.007}_{-0.008}$
$1608.0(\frac{49}{2})$	$0.996^{+0.10}_{-0.10}$	$0.222^{+0.044}_{-0.044}$	$0.034^{+0.007}_{-0.007}$
Band 6			
$728.9(\frac{31}{2})$	$2.577^{+0.14}_{-0.15}$	$1.902^{+0.221}_{-0.206}$	$0.208^{+0.022}_{-0.024}$
$952.3(\frac{35}{2})$	$2.257^{+0.04}_{-0.05}$	$0.631^{+0.028}_{-0.022}$	$0.165^{+0.006}_{-0.007}$
$1133.2(\frac{39}{2})$	$1.994^{+0.04}_{-0.05}$	$0.332^{+0.016}_{-0.013}$	$0.131^{+0.005}_{-0.006}$
$1352.8(\frac{43}{2})$	$1.766^{+0.04}_{-0.06}$	$0.170^{+0.011}_{-0.008}$	$0.106^{+0.005}_{-0.007}$
$1552.5(\frac{47}{2})$	$1.131^{+0.09}_{-0.09}$[a]	$0.205^{+0.032}_{-0.032}$[a]	$0.044^{+0.007}_{-0.007}$[a]

[a]Effective value.

IV. DISCUSSION

The positive-parity band structure in ^{107}Cd is built upon a low-Ω $g_{7/2}$ neutron orbital [9]. The development of the signature partner bands 5 and 6 are due to the alignment of a pair of low-Ω $h_{11/2}$ neutrons with a crossing frequency of $\hbar\omega = 0.42$ MeV [9]. The signature partner bands 5 and 6 appear to be based on the $\pi(g_{9/2}^{-2}) \otimes \nu(g_{7/2}h_{11/2}^2)$ configuration after the crossing. The aligned neutrons add up to give the total neutron angular momentum vector $\vec{J}_\nu$. The generation of high spin states in these bands are interpreted to be due to the closing of a pair of high-Ω $g_{9/2}$ proton hole vectors, $\vec{j}_{\pi_1}$ and $\vec{j}_{\pi_2}$, which are nearly perpendicular to the neutron angular momentum vector at the bandhead.

The semiclassical model, initially developed by Macchiavelli *et al.* [20,21] for magnetic rotation, was extended by Sugawara *et al.* [22] for AMR bands. A slightly modified version used by us for ^{105}Cd [2] has been used here to explain the observed properties of the positive-parity bands 5 and 6 of ^{107}Cd. We consider the coupling of three neutron particles and two proton holes. With six possible proton-neutron pairs and one possible proton-proton pair, the total energy is given by

$$E(I) = \frac{\left(I - \vec{j}_{\pi_1} - \vec{j}_{\pi_2} - \vec{J}_\nu\right)^2}{2\Im} + V\left(\frac{3\cos^2\theta - 1}{2}\right) - \frac{V'}{6}\left(\frac{3\cos^2(2\theta) - 3}{2}\right). \quad (1)$$

Here, the magnitude of the effective interaction of a hole-hole (proton-proton) pair (v_{pp}) has been considered to be 1/6 times that of a particle-hole (neutron-proton) pair (v_{np}). $V = 6v_{np}$ and $V' = \frac{1}{6}V$. $\Im$ is the moment of inertia of the core and θ is the angle between the proton and neutron blades. The sign of v_{np}, V being positive and that of v_{pp}, V' being negative, make the last term of Eq. (1) negative. On setting $(\frac{dE}{d\theta})_I = 0$ and

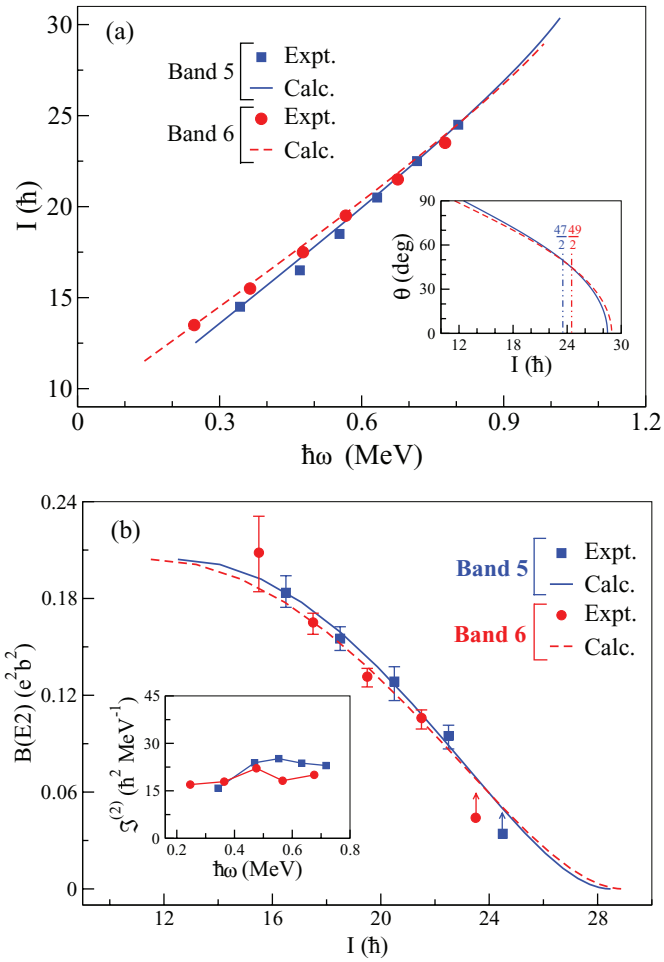

FIG. 3. (Color online) Comparison of the measured I vs ω (a) and $B(E2)$ vs I (b) values for bands 5 and 6 with those calculated from the SCM.

considering $j_{\pi_1} = j_{\pi_2} = j_\pi$, we obtain

$$I = \{2j_\pi\cos\theta + 3j_\nu\} + \frac{3\Im}{2j_\pi}\cos\theta\left[V - \frac{2}{3}V'\cos(2\theta)\right], \quad (2)$$

$$\omega = \frac{3}{2j_\pi}\cos\theta\left[V - \frac{2}{3}V'\cos(2\theta)\right]. \quad (3)$$

We interpret the bands 5 and 6 as based on the same configuration but having different signature neutron orbitals. The R_π symmetry [1] around $\vec{J}_\nu$ breaks, hence giving rise to two distinct AMR bands with very weak M1 connections. For band 5, $J_\nu = 25/2$. The calculated I vs ω values are compared with the empirical values after adding a constant core contribution of $\omega_0 = 0.242$ MeV, which corresponds to the angular momentum contribution in the curly brackets in Eq. (2). An excellent agreement is obtained for $\Im = 10\hbar^2$ MeV^{-1}, $V = 2.36$ MeV, as shown in Fig. 3(a). For band 6, $J_\nu = 23/2$. An excellent agreement is again obtained between the calculated and empirical I vs ω values [Fig. 3(a)] for $\omega_0 = 0.143$ MeV, $\Im = 10h^2$ MeV^{-1}, and $V = 2.8$ MeV. $j_\pi = 9/2$ for both bands 5 and 6. These results for the I vs ω values support our interpretation of the aforementioned configuration for the signature partner bands 5 and 6 and that

the generation of high spin states in both these bands is due to the twin-shears mechanism, i.e., AMR.

Within the SCM description of the twin-shears mechanism for AMR, the $B(E2)$ values can be written as

$$B(E2) = \frac{15}{32\pi}(eQ)^2_{\text{eff}} \sin^4\theta. \quad (4)$$

The $B(E2)$ values, calculated at different spins for the bands 5 and 6, using the θ values from Eq. (2) and $(eQ)_{\text{eff}} = 1.17eb$, agree well with the experimentally obtained values [Fig. 3(b)]. A similar behavior of I vs ω and $B(E2)$ vs I in the two bands confirms that the bands are based on the same nuclear structure and differ slightly in spin alignments. The behavior of the shear angle θ as a function of spin [see insert of Fig. 3(a)] shows that there is a similar closing of the proton blades towards the neutron angular momentum vector, generating high spin states in both bands 5 and 6. The n-p closing angle of about $45^\circ - 50^\circ$ at the highest observed spin implies that the twin shears have not closed completely. For both the bands, the $\Im^{(2)}$ values remain nearly constant with spin and rotational frequency [insert of Fig. 3(b)], which is another important feature of AMR.

Since the positive-parity bands 5 and 6 originate after the band crossing with the alignment of a pair of $h_{11/2}$ neutrons, the bands become yrast at higher deformation. For both the bands, the nucleus has moderate quadrupole deformation near the bandhead, indicated by the extracted β_2 values 0.19 and 0.20 at spins $33/2^+$ and $31/2^+$, respectively. The experimentally obtained Q_t and hence the β_2 values are found to be decreasing with increasing spin for both bands 5 and 6 of ^{107}Cd. For band 5, the measured β_2 values decrease from $\beta_2 = 0.19$ at spin $33/2^+$ to $\beta_2 = 0.13$ at spin $45/2^+$. For band 6, the β_2 values decrease from $\beta_2 = 0.20$ at spin $31/2^+$ to $\beta_2 = 0.14$ at spin $43/2^+$ Hence, with the gradual closing of the proton angular momentum blades towards the neutron angular momentum vector, the nucleus, from a nearly prolate moderate deformation, gradually heads towards a nearly spherical shape high up the band. This is true for both bands 5 and 6.

V. SUMMARY

To summarize, we have measured the lifetimes of the high spin states (above $27/2^+$) in a pair of positive-parity bands 5 and 6 of the odd-A ^{107}Cd nucleus by using the Doppler-shift attenuation method. The decreasing trend in the empirical $B(E2)$ values with increase in spin has been interpreted by the semiclassical model for AMR bands using the proposed configuration $(\nu g_{7/2} h^2_{11/2} \otimes \pi g^{-2}_{9/2})$. Generation of high spin states beyond spin $23/2^-$ occurs due to the gradual closing of the proton vectors towards the aligned neutron vectors along with some contribution from the core. The observed rapidly decreasing $B(E2)$ values with increasing spin along with nearly constant $\Im^{(2)}$ $[\sim 20\hbar^2\,\text{MeV}^{-1}]$ and large $\Im^{(2)}/B(E2)$ ratio $(>100\hbar^2\,\text{MeV}^{-1}(eb)^{-2})$ increasing with spin, for both bands 5 and 6, establish that the bands are examples of AMR bands. The R_π symmetry breaking is evident in the observation of two AMR bands based on signature partner configuration and having different alignments.

The experimental findings supported by the SCM calculations provide the first evidence of two AMR bands in any nucleus, and the work opens up the possibility of discovering more than one AMR band in a single nucleus and also in signature partner bands.

ACKNOWLEDGMENTS

The authors thank Prof. S. Frauendorf (Notre Dame) for very useful discussions and suggestions. The accelerator staff at TIFR, Mumbai, and the help provided by Dr. Vandana Nanal are highly acknowledged. Our special thanks to Prof. D. Tonev (LNL/Sofia) and IUAC, New Delhi, for providing us the target. Financial support from the Department of Science and Technology, the Department of Atomic Energy, and the Ministry of Human Resource Development (Government of India) is also gratefully acknowledged.

[1] S. Frauendorf, Rev. Mod. Phys. **73**, 463 (2001).
[2] D. Choudhury *et al.*, Phys. Rev. C **82**, 061308(R) (2010).
[3] A. K. Jain and D. Choudhury, Pramana: J. Phys. **75**, 51 (2010).
[4] A. J. Simons *et al.*, Phys. Rev. Lett. **91**, 162501 (2003).
[5] A. J. Simons *et al.*, Phys. Rev. C **72**, 024318 (2005).
[6] P. Datta *et al.*, Phys. Rev. C **71**, 041305 (2005).
[7] S. Roy *et al.*, Phys. Lett. B **694**, 322 (2011).
[8] P. W. Zhao, J. Peng, H. Z. Liang, P. Ring, and J. Meng, Phys. Rev. Lett. **107**, 122501 (2011).
[9] Dan Jerrestam *et al.*, Nucl. Phys. A **545**, 835 (1992).
[10] R. Palit, AIP Conf. Proc. **1336**, 573 (2011).
[11] R. Palit *et al.*, Nucl. Instrum. Methods Phys. Res., Sect. A **680**, 90 (2012).
[12] H. Tan *et al.*, in *Nuclear Science Symposium Conference Record NSS 08* (IEEE, Washington, DC, 2008), p. 3196.
[13] DAMM: Milner Package, the Oak Ridge analysis software (private communication).
[14] R. Palit (private communication).
[15] D. C. Radford, Nucl. Instrum. Methods. A **361**, 297 (1995).
[16] J. C. Wells and N. R. Johnson, ORNL Physics Division Progress, Report No. ORNL-6689, September 30, 1991.
[17] D. Choudhury *et al.* (unpublished).
[18] L. C. Northcliffe and R. F. Schilling, Nucl. Data Tables **A7**, 233 (1970).
[19] F. James and M. Roos, Comput. Phys. Commun. **10**, 343 (1975).
[20] A. O. Macchiavelli *et al.*, Phys. Rev. C **57**, R1073 (1998); **58**, 3746 (1998).
[21] R. M. Clark and A. O. Macchiavelli, Annu. Rev. Nucl. Part. Sci. **50**, 1 (2000).
[22] M. Sugawara *et al.*, Phys. Rev. C **79**, 064321 (2009).